



RANS MODELS APPLIED IN A FLOW OVER A ROUNDED EDGE

Wendel Rodrigues Miranda

Department of Mechanical Engineering, IME, 22290-270, Rio de Janeiro, RJ, Brazil
eng.wndl@gmail.com

André Luiz Tenório Rezende

Department of Mechanical Engineering, IME, 22290-270, Rio de Janeiro, RJ, Brazil
arezende@ime.eb.br

Abstract. *The purpose of this study is a numerical prediction of the separation bubble in a steady state flow over a 2D half-body by two RANS models: k - ω SST and Spalart-Allmaras. This numerical simulation technique uses a reduced computational data and has been adopted for most practical engineering problems, since the design of such applications relies on the steady stateflow and average velocity field. The main purpose is to analyze the flow dynamics of the recirculation bubble for dimensionless parameter $\eta = R/H$ (ratio of rounded radius and body height). One case is investigated, corresponding to $\eta = 0.25$. The Reynolds number, based on the free stream velocity U_∞ and the height of the obstacle H , is equal to $Re = 2000$. These RANS models assume isotropic modeling of the Reynolds tensor. The results are compared with experimental and computational data.*

Keywords: *separation bubble, Reynolds Averaged Navier-Stokes simulation (RANS), reattachment.*

INTRODUCTION

In many practical situations of engineering, flow separation is triggered by a sharp edge. In the context of robust bodies, the edges may advantageously be smoothed to improve the aerodynamic characteristics of the body as well as controlling the production of vibrations and noise. Despite the practical knowledge of this type of influence (especially in the automotive industry), there is no clear understanding of the physical mechanisms involved in the change of the resulting flow separation depending on the shape of the edge. In this work, the goal is to study the formation of a separation bubble considering a generic configuration where the flow separates over a rounded edge. The change in the dynamics of this effect will be analyzed through the influence of: (i) the mean flow (the characteristics of the formation of the bubble separation), (II) the production of turbulent energy, (iii) the effects with respect to perturbations in free stream. (Lamballais *et al*, 2010).

2 MATHEMATICAL MODEL

The Reynolds-averaged approach is based on decomposing the velocity as $u = \bar{u} + u'$, where u is the average velocity vector and u' the velocity vector fluctuation. The average continuity and momentum equation (RANS), for a steady state incompressible flow is given by:

$$\nabla \cdot \bar{u} = 0 \quad (1)$$

$$\nabla \cdot (\bar{u}\bar{u}) = -\nabla \left(\frac{p}{\rho} \right) + \nu \nabla^2 + \nabla \cdot (-\overline{u'u'}) \quad (2)$$

where:

ρ = density;

$\nu = \mu/\rho$ is the cinematic viscosity;

μ = is the molecular or dynamic viscosity;

p = is the pressure.

Equation (2) has the same form of the Navier-Stokes equation, but now it has an additional term, the turbulent Reynolds Stress term, $-\overline{u'u'}$, representing the influence the influence of the fluctuation on the average flow. In order to close Eq. (2), the turbulent Reynolds stress can be modeled based on the Boussinesq hypothesis, where the turbulent stress is obtained through an analogy with Stokes law, i.e., the stress is proportional to the deformation rate. The turbulence models selected to be investigated at the present work are described next.

2.1 SST κ - ω MODEL

The turbulent Reynolds stress is modeled as:

$$-\overline{u'u'} = \nu_t (\nabla \bar{u} + \nabla \bar{u})^T - \frac{2}{3} \kappa \delta \quad (3)$$

where κ is the turbulent kinetic energy and ν_t is the turbulence viscosity, which is defined in accordance with the Shear-Stress Transport (SST) κ - ω model (Menter *et al*, 2003). This model was proposed for aeronautical flows simulations with strong adverse pressure gradients and separation with the best behavior of the κ - ε and κ - ω models. For boundary layers flows, the κ - ω model is superior to the k - ε model in the solution of the viscous near-wall region, and has been successful in problems involving adverse pressure gradients. Nevertheless, the κ - ω model requires a non-zero boundary condition on ω for non-turbulent free stream, and the calculated flow is very sensitive to the value specified (Menter, 1992). It has also been show (Cazalbou *et al*, 1993) that the κ - ε model does not suffer this deficiency.

Thus, the SST model blends the robust and precise formulation of the κ - ω model close to walls with the free stream independence of the κ - ε model outside the boundary layer. To accomplish this, the κ - ε model is written in terms of ω . Then the standard κ - ω model and the transformed κ - ε model are both multiplied by a blending function and both models are added together. This blending function F_1 is zero (leading to the standard κ - ω model) at the inner edge of a turbulent boundary layer and blend to a unitary value (corresponding to the standard κ - ε model) at the outer edge of the layer. Therefore the turbulent kinetic energy κ and specific dissipation rate ω of the SST model is given by (Menter *et al*, 2003)

$$\frac{\partial \kappa}{\partial t} + \bar{u}_i \frac{\partial \kappa}{\partial x_i} = \bar{P}_\kappa - \beta^* \kappa \omega + \frac{\partial}{\partial x_j} \left[(v + \sigma_\kappa \nu_t) \frac{\partial \kappa}{\partial x_j} \right] \quad (4)$$

$$\frac{\partial \omega}{\partial t} + \bar{u}_i \frac{\partial \omega}{\partial x_i} = \alpha S^2 - \beta \omega^2 + \frac{\partial}{\partial x_j} \left[(v + \sigma_\kappa \nu_t) \frac{\partial \kappa}{\partial x_j} \right] + (1 - F_1) 2\sigma_d \frac{1}{\omega} \frac{\partial \kappa}{\partial x_j} \frac{\partial \omega}{\partial x_j} \quad (5)$$

The last term in right side of Eq. (5) is known as cross diffusion term. Menter (1992) demonstrated that introducing cross diffusion term in the ω equation, the free stream dependency of the κ - ω model is reduced. The main effect of cross diffusion in free-shear flows is to increase the production of ω , which consequently increases the dissipation of κ . In the Eq. (5) the cross diffusion is multiplying by blending function F_1 based upon the distance to the nearest wall. As explained previously, F_1 is equal to zero in the far field (κ - ε model), and switches over to one inside the boundary layer (κ - ω model). The blending function F_1 is defined as:

$$F_1 = \tanh(\text{arg}_1^4) \quad (6)$$

$$\text{arg}_1 = \min \left[\max \left(\frac{\sqrt{k}}{\beta^* \omega y}, \frac{500v}{y^2 \omega} \right); \frac{4\rho \sigma_\omega z k}{CD_{k\omega} y^2} \right] \quad (7)$$

where y is the distance to the nearest surface and $CD_{k\omega}$ is the positive portion of the cross diffusion term, given for:

$$CD_{k\omega} = \max \left(2\rho \sigma_d \frac{1}{\omega} \frac{\partial \kappa}{\partial x_j} \frac{\partial \omega}{\partial x_j}; 10^{-10} \right) \quad (8)$$

The definition of the turbulent eddy viscosity provides a better treatment of the transport of turbulent shear-stress in adverse pressure gradient boundary layers. This definition is based on Bradshaw's hypothesis that in boundary layer flows the Reynolds shear stress is proportional to the turbulent kinetic energy. The turbulent eddy viscosity is formulated as follows:

$$\nu_t = \frac{\alpha_1 k}{\max(\alpha_1 \omega; S F_2)} \quad (9)$$

where S is the modulus of the mean rate-of-strain tensor S_{ij} ,

$$S = \sqrt{2S_{ij}S_{ij}} \quad (10)$$

$$S_{ij} = \frac{1}{2} \left(\frac{\partial \bar{u}_i}{\partial x_j} + \frac{\partial \bar{u}_j}{\partial x_i} \right) \quad (11)$$

and F_2 is the blending function for the turbulent eddy viscosity in the SST model, defined as:

$$F_2 = \tanh(\arg_2^2) \quad (12)$$

$$\arg_2 = \max \left(\frac{\sqrt{k}}{\beta^* \omega y}; \frac{500\nu}{y^2 \omega} \right) \quad (13)$$

In the SST model the production of turbulence kinetic energy is limited to prevent the build-up of turbulence in stagnation regions as:

$$\tilde{P}_k = \min(v_t S^2; 10\beta^* k \omega) \quad (14)$$

Let ϕ represent the set of closure constants for the SST model and let ϕ_1 and ϕ_2 represent the constants from the standard $\kappa\text{-}\omega$ and $\kappa\text{-}\varepsilon$ models respectively. The constants ϕ are calculated using a blend between the constants ϕ_1 ($\kappa\text{-}\omega$) and ϕ_2 ($\kappa\text{-}\varepsilon$), which can be seen in Table 1, as:

$$\Phi = F_1 \Phi_1 + (1 - F_1) \Phi_2 \quad (15)$$

Table 1 -Closure coefficients of the SST model.

	β	β^*	σ_κ	σ_ω	σ_d	α
ϕ_1 (standard $\kappa\text{-}\omega$)	0.075	0.09	0.5	0.5	0.856	5/9
ϕ_2 (standard $\kappa\text{-}\varepsilon$)	0.0828	0.09	1.0	0.856	0.856	0.44

2.2 SPALART-ALLMARAS MODEL

Developed by Spalart and Allmaras (1992), this is a model relatively simple that solves a transport differential equation for the turbulent viscosity and, therefore, it requests smaller computational effort. The Spalart-Allmaras model was designed specifically for aerospace applications involving wall-bounded flows and adverse pressure gradients. The differential equation is derived by using empiricism, arguments of dimensional analyses and selected dependence on the molecular viscosity. For this model, the turbulent Reynolds stress is modeled without the last term of Eq. (3), as:

$$-\overline{u'u'} = \nu_t (\nabla \bar{u} + \nabla \bar{u})^T \quad (16)$$

The eddy viscosity is defined as

$$\nu_t = \tilde{\nu} f_{v1} \quad (17)$$

where f_{v1} is a viscous damping function used to treat more appropriate the buffer layer and viscous sublayer, computed as

$$f_{v1} = \frac{x^3}{x^3 + C_{v1}^3} \quad ; \quad x = \frac{\tilde{\nu}}{\nu} \quad (18)$$

The transport equation for the working variable $\tilde{\nu}$ is given by (Deck et al, 2002)

$$\frac{\partial \tilde{\nu}}{\partial t} + \frac{\partial(\bar{u}_i \tilde{\nu})}{\partial x_j} = G_\nu + \frac{1}{\sigma \tilde{\nu}} \left\{ \frac{\partial}{\partial x_j} \left[(\nu + \tilde{\nu}) \frac{\partial \tilde{\nu}}{\partial x_j} \right] + C_{b2} \left(\frac{\partial \tilde{\nu}}{\partial x_j} \right)^2 \right\} - Y_\nu \quad (19)$$

In the Eq. (19), G_ν is the production term. Dacles-Mariani *et al* (1995) combine the effects of the rotation and strain tensors in the definition of production of ν_t , in order to avoid overestimation of the turbulent viscosity, in regions where the vorticity measure exceeds the strain rate. G_ν is based on a modification on the vorticity magnitude Ω in order to maintain its log-layer behavior, where Ω_{ij} is the mean rate-of-rotation tensor.

W. Miranda, A. Rezende

Reynolds Averaged Navier-Stokes (RANS) Numerical Simulation of a Separation Bubble on a Rounded Edge

$$G_v = C_{b1} \tilde{\Omega} \tilde{v} \quad ; \quad \tilde{\Omega} = \Omega + \frac{\tilde{v}}{k^2 d^2} f_{v2} + C_{prod} \min(0, S - \Omega) \quad (20)$$

$$\Omega_{ij} = \frac{1}{2} \left(\frac{\partial \bar{u}_i}{\partial x_j} - \frac{\partial \bar{u}_j}{\partial x_i} \right) \quad , \quad \Omega = \sqrt{2 \Omega_{ij} \Omega_{ij}} \quad (21)$$

where d is the wall distance, $C_{prod} = 2.0$ and f_{v2} is a damping function, given by

$$f_{v2} = 1 - \frac{x}{1 + x f_{v1}} \quad (22)$$

The destruction term Y_v is

$$Y_v = C_{w1} f_w \left(\frac{\tilde{v}}{d} \right)^2 \quad , \quad f_w = g \left[\frac{1 + C_{w3}^6}{g^6 + C_{w3}^6} \right]^{1/6} \quad , \quad g = r + C_{w2} (r^6 - r) \quad , \quad r = \frac{\tilde{v}}{\tilde{\Omega} k^2 d^2} \quad (23)$$

The empiric constants of the model are: $C_{b1} = 0.1355$; $C_{b2} = 0.622$; $C_{w1} = C_{b1} / \kappa^2 + (1 + C_{b2}) / \sigma_{\tilde{v}}$; $C_{w2} = 0.3$; $C_{w3} = 2.0$; $C_{v1} = 7.1$; $\sigma_{\tilde{v}} = 2/3$; $k = 0.41$.

3 RESULTS

The figure 1 shown a flow over a semi-infinity bi-dimensional body with a rounded edge located at stagnation point $(x,y) = (x_s, 0)$, with $x_s = 16H$. The geometry of body is defined by height H and radius R of the rise, originating the dimensionless parameter $\eta = R/H$, that in this case $\eta = 0.25$ (Coutine and Spohn, 2004). Using as reference parameter the upstream velocity U_∞ , the Reynolds number can be defined as $Re = U_\infty H / \nu$, ($Re = 2000$) (Lamballais *et al*, 2010). Thus the flow in an infinity domain, free of any disturbance is defined only by the parameters η e Re .

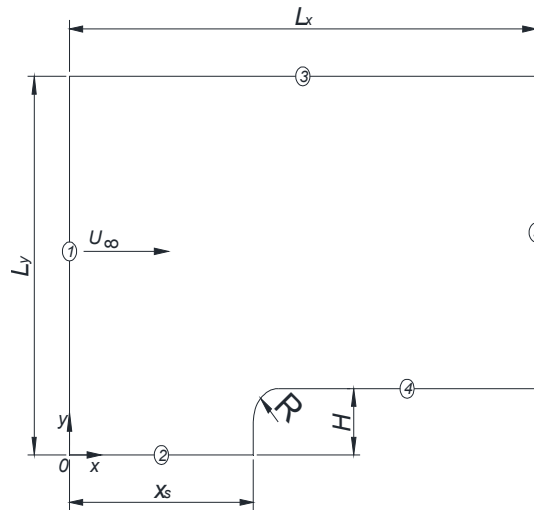


Figure 1 – Flow configuration

The boundary conditions in the regions 1, 2 and 3 is the stream velocity is $(U_\infty, 0, 0)$. In region 4, relating the step and the wall, the conditions are $u_{wall} = v_{wall} = 0$. In the downstream flow region 5, the gauge pressure is prescribed as being the atmospheric pressure.

The computational domain is $L_x \times L_y = 41.25 H \times 11 H$. The result mesh is structured in rectangular coordinates (x and y direction) and has 168169 nodes. The distance of first node above the plate was designed $10^{-2} H$ (H is the height of rounded edge) to guarantee $y^+ = (\tau_s / \rho)^{0.5} y / \nu$ around 1, which is the value recommended for both RANS, where τ_s is the wall shear stress. To eliminate the false diffusion effect a mesh orthogonal to mean flow was selected (see figure 2a and 2b), instead of the curved used by Yang & Voke (2001).

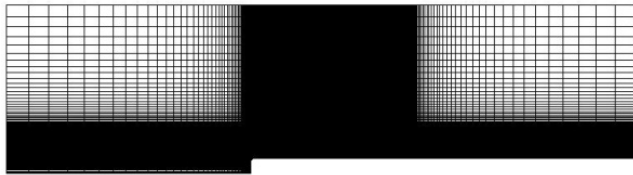


Figure 2a – Structured Mesh

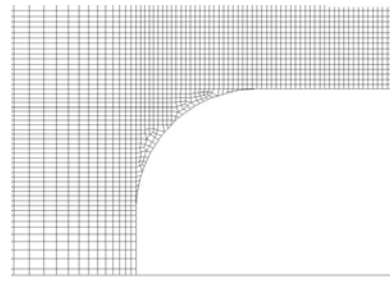


Figure 2b – Structured Mesh – rounded region.

In the region very near the radius was chosen an irregular structure for closing the mesh. In this same region was guaranteed amount of 20 nodes equally spaced by the curvature.

To inlet mean velocity U_∞ was introduced the inflow perturbations: $u' = 0.1\% U_\infty$ e $1\% U_\infty$ (Lamballais *et al*, 2010) to observe the effects on reattachment length.

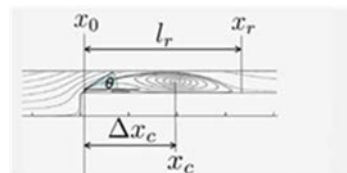
The solution of flow field was performed by commercial software FLUENT®. This code is based in Finite Volume Method. The simulation was obtained with the scheme SIMPLE to the pressure-velocity coupling and QUICK scheme (Leonard, 1979) for interpolation function. The problem was considered converged when the residue was lower than 10^6 .

3.1 REATTACHMENT LENGHT

The tables 1, 2 and 3 show the reattachment length l_r , normalized to mean velocities with inflow perturbations $u' = 0\% U_\infty$ and $0.1\% U_\infty$ obtained by turbulence methods. Tables 2 and 3 are compared to previous works in 2D and 3D of Lamballais *et al* (2010).

Table 2 – Inflow perturbation of $1\% U_\infty$.

	$\kappa\text{-}\omega$ SST 2D	S-A 2D
l_r	6.49	1.91
$\Delta x_c / l_r$	0.39	0.32
U_{min}	-0.28	-0.58

Figure 3 – l_r representation (Lamballais *et al*, 2010)Table 3 – Inflow perturbation of $0.1\% U_\infty$ and DNS 2D and 3D.

	$\kappa\text{-}\omega$ SST 2D	S-A 2D	DNS 2D Lamballais <i>et al</i> (2010)	DNS 3D Lamballais <i>et al</i> (2010)
l_r	7.03	4.38	3.4	5.8
$\Delta x_c / l_r$	0.42	0.37	0.54	0.62
U_{min}	-0.28	-0.47	-0.38	0.34

Table 4 – Inflow perturbation of $0\% U_\infty$ and DNS 2D and 3D

	$\kappa\text{-}\omega$ SST 2D	S-A 2D	DNS 2D Lamballais <i>et al</i> (2010)	DNS 3D Lamballais <i>et al</i> (2010)
l_r	6.98	6.34	3.3	7.4
$\Delta x_c / l_r$	0.42	0.47	0.56	0.67
U_{min}	0.28	0.41	0.39	0.34

The results obtained with the model $\kappa\text{-}\omega$ SST are better than the model Spalart-Allmaras. This is due to the fact that the SA model is designed for aerodynamics applications with high Reynolds numbers. The Spalart-Allmaras results show be quite sensitive to the variation of the disturbance in the free stream velocity.

3.2 MEAN STREAMLINES

Figures 4 to 9 show the mean streamlines for both models $k-\omega$ SST and Spalart-Allmaras with inflow perturbations $u' = 1\%$, $u' = 0.1\% U_\infty$ and $U_\infty u' = 0\%$.

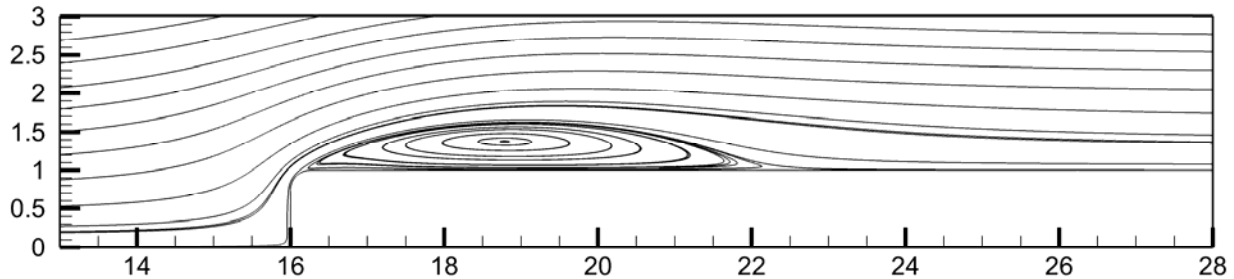


Figure 4 – Mean streamlines for $k-\omega$ SST model. Inflow perturbation $u' = 1\% U_\infty$.

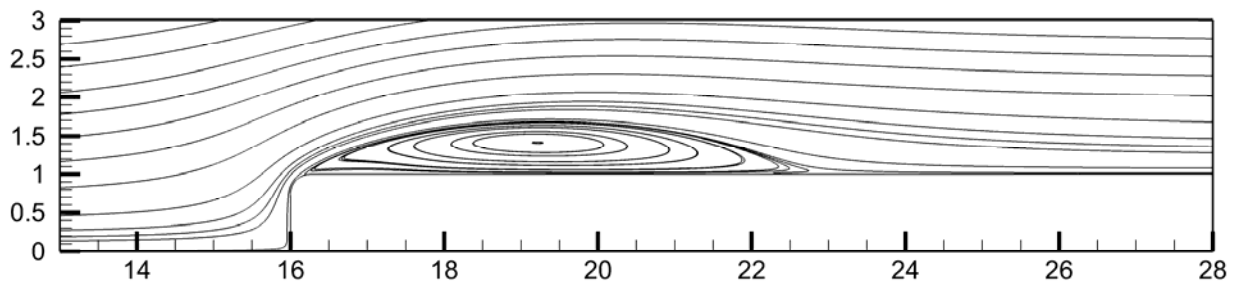


Figure 5 – Mean streamlines for $k-\omega$ SST model. Inflow perturbation $u' = 0.1\% U_\infty$.

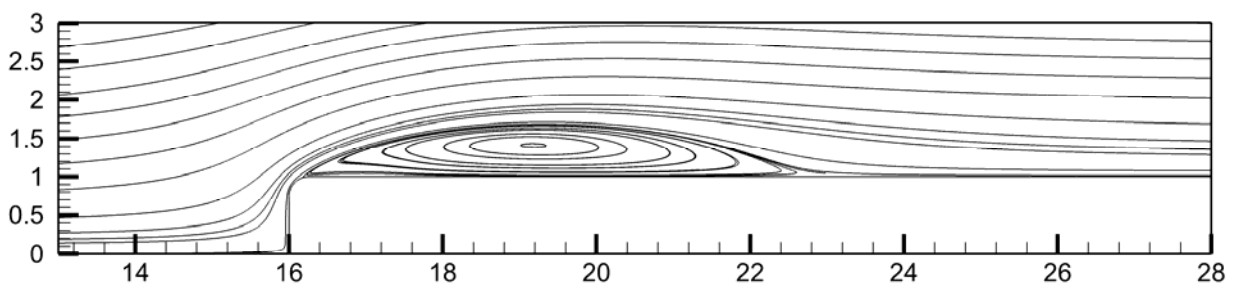


Figure 6 – Mean streamlines for $k-\omega$ SST model. Inflow perturbation $u' = 0\% U_\infty$.

The results of $k-\omega$ SST model are very close to results of 3D DNS of Lamballais *et al* (2010). The relative error was 21.2% and -5.4% for inflow perturbations of 0.1 and 0% U_∞ , respectively.

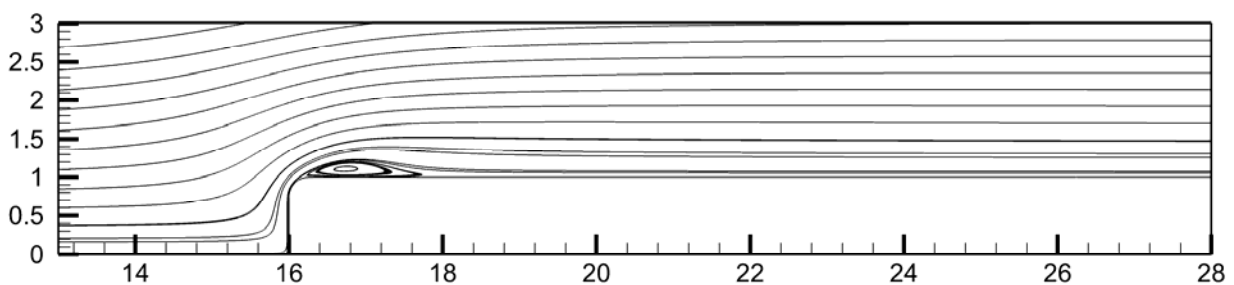
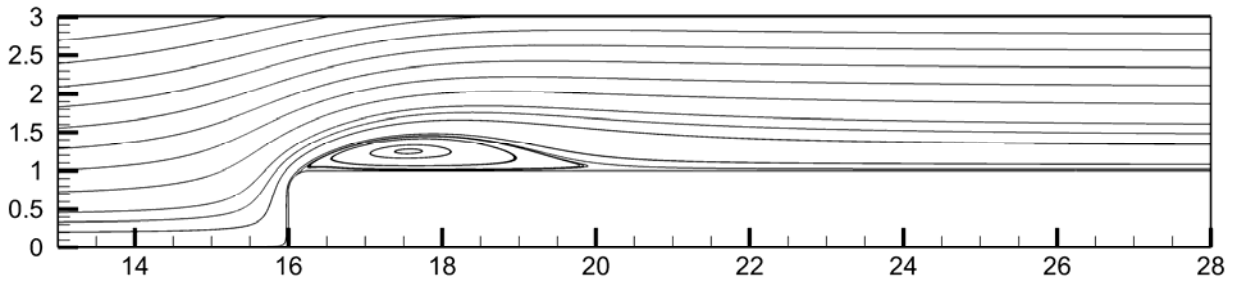
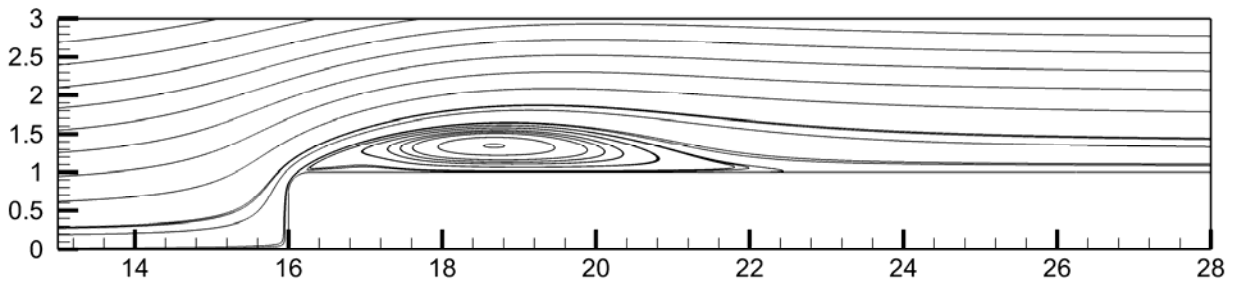


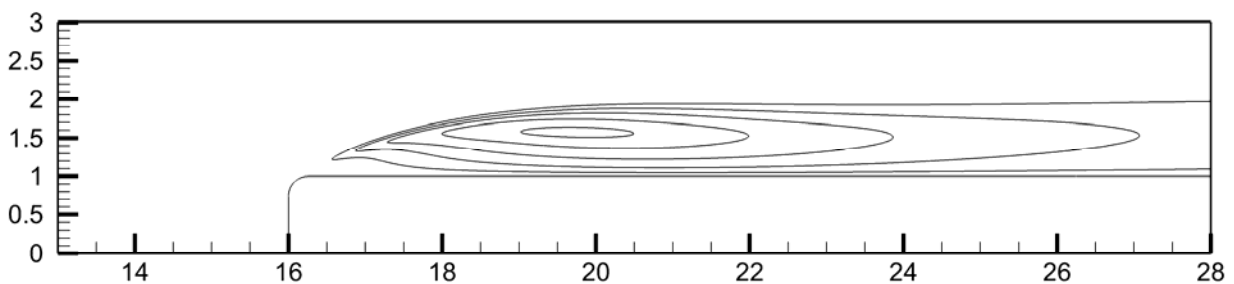
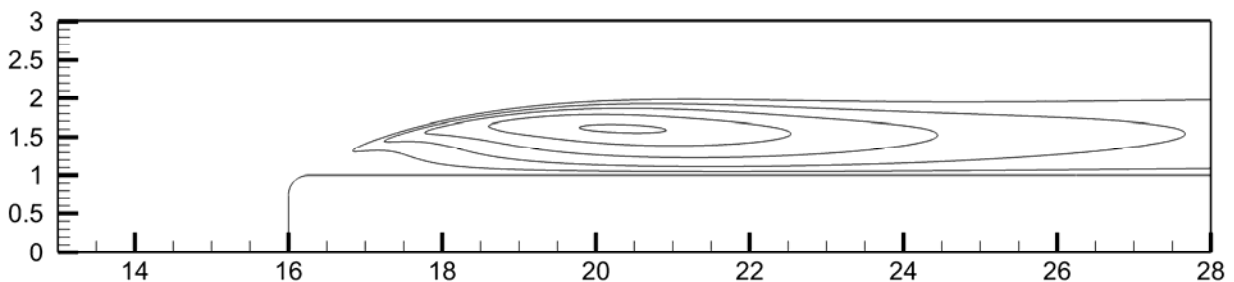
Figure7 – Mean streamlines for Spalart-Allmaras model. Inflow perturbation $u' = 1\% U_\infty$.

Figure 8 – Mean streamlines for Spalart-Allmaras model. Inflow perturbation $u' = 0.1\% U_\infty$.Figure 9 – Mean streamlines for Spalart-Allmaras model. Inflow perturbation $u' = 0\% U_\infty$.

The Spalart-Allmaras model is not adequate for low Reynolds number. Because the model is dissipative the reattachment length decrease when inflow perturbation increases. In work of Rezende et al (2007) this effect was not observed, because the Reynolds number used was 2.13×10^5 .

3.3 TURBULENT KINETIC ENERGY K CONTOURS

To have a better idea about the location of the main unsteady regions of the flow, turbulent kinetic energy contours are presented in Figs. 10, 11 and 12 for $k-\omega$ SST model.

Figure10 – Turbulent kinetic energy k contours for $k-\omega$ SST model. Inflow perturbation $u' = 1\% U_\infty$ ($k = 1\% U_\infty^2$)Figure11 – Turbulent kinetic energy k contours for $k-\omega$ SST model. Inflow perturbation $u' = 0.1\% U_\infty$ ($k = 1\% U_\infty^2$)

W. Miranda, A. Rezende

Reynolds Averaged Navier-Stokes (RANS) Numerical Simulation of a Separation Bubble on a Rounded Edge

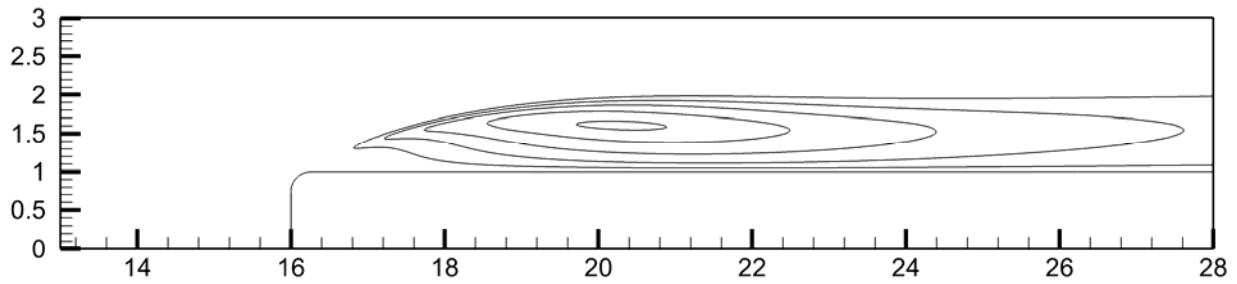


Figure12 – Turbulent kinetic energy k contours for k - w SST model. Inflow perturbation $u' = 0\% U_\infty$ ($k = 1\% U_\infty^2$)

Qualitatively, similar patterns are obtained from k - w SST model with different inflow perturbations, with a simple shifting of the contours further downstream.

3.4 PRESSURE DISTRIBUTION CONTOUR

The pressure distribution is analyzed through the pressure coefficient defined as:

$$C_p = \frac{(p_\infty - p)}{(0.5\rho U_\infty^2)} \quad (24)$$

Where p is the static pressure, p_∞ and U_∞ are the free stream pressure and velocity.

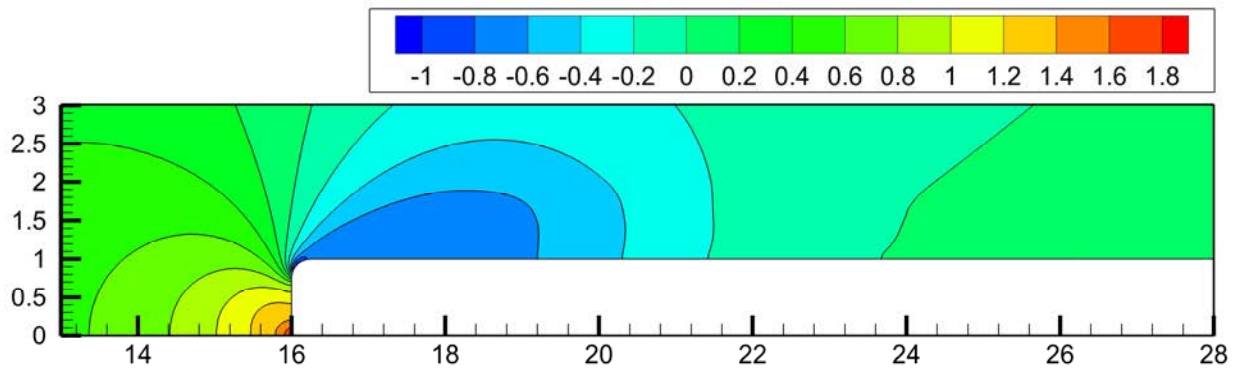


Figure13 – Pressure contours for k - w SST model. Inflow perturbation $u' = 1\% U_\infty$.

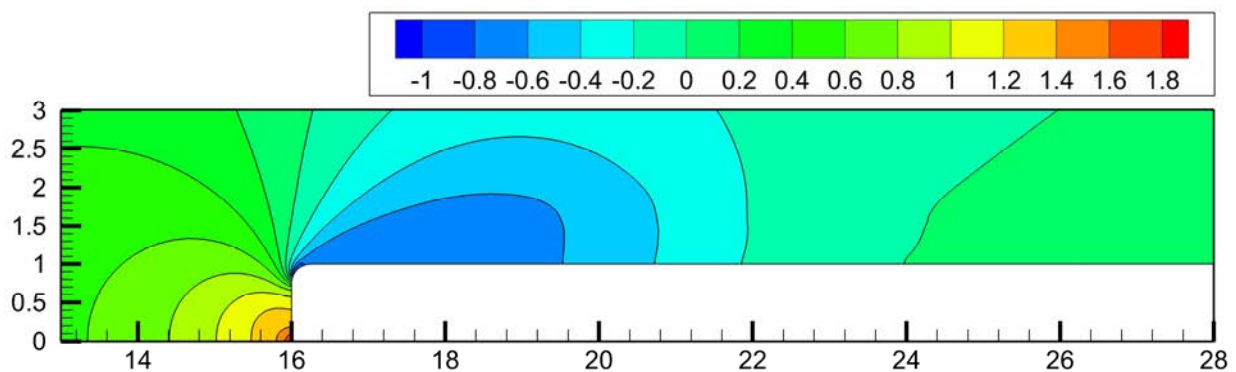


Figure14 – Pressure contours for k - w SST model. Inflow perturbation $u' = 0.1\% U_\infty$.

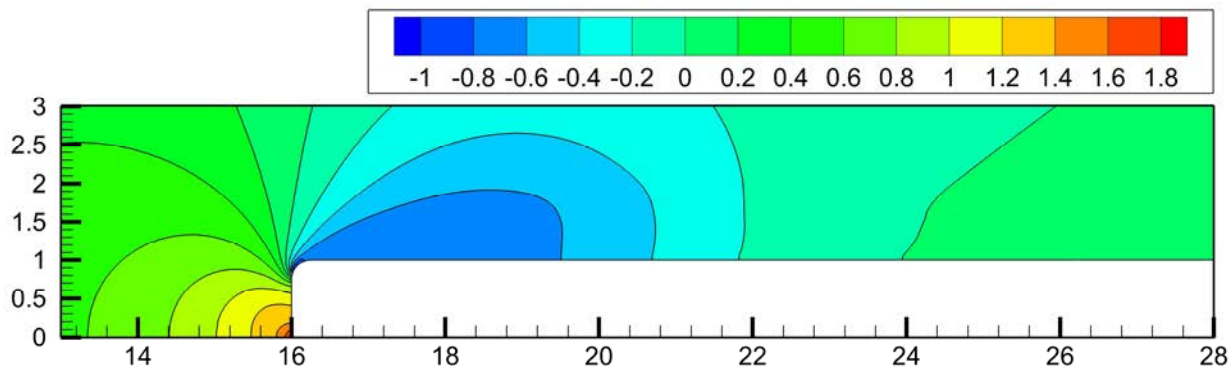


Figure15 – Pressure contours for $k-w$ SST model. Inflow perturbation $u' = 0\% U_\infty$.

The bubble recirculation region has low pressure gradient. In this region the velocity profile is higher. The stagnation point x_s (16 H) has a higher pressure gradient and lower velocity.

4 CONCLUSION

The objective of this research was to study the formation of a separation bubble over a 2D half-body by Reynolds Averaged Navier-Stokes (RANS) simulation.

The Spalart-Allmaras model was not adequate for this work, the Reynolds number used was low ($Re = 2000$).

The results of $k-w$ SST model were very close to results of 3D DNS of Lamballais *et al* (2010).

The mean streamlines presented reasonable agreement with compared work results.

The pressure contour with higher value indicates regions with lower velocity. The pressure contour with lower values indicates regions with higher velocity.

The numerical simulation $k-w$ SST technique uses a reduced computational data and can be applied for most practical engineering problems, since the design of such applications relies on the steady stateflow and average velocity field. There was no restriction about low Reynolds number.

The visualization of 3D transition encourage the investigation with more demanding models such as LES.

5 ACKNOWLEDGEMENTS

The authors acknowledge the support awarded to this research by the Brazilian Research Coordinate, CAPES.

6 REFERENCES

- Araújo, F., Rezende, A.L.T., Nieckele, A.O., (2011). "Influence of the Angle of Attack on the leading Edge Bubble in a Flow over a Thin Flat Plate" 21st International Congress of Mechanical Engineering COBEM 2011.
- Cazalbou, J.B., Spalart, P.R., Bradshaw, P., 1993, "On the Behavior of 2-Equation Models at the Edge of a Turbulent Region", *Physics of Fluids*, Vol. 6, No. 5, pp. 1797-1804.
- Courtine, S., Spohn, A. (2003). "Formation of Separation Bubbles on Rounded" in *Proceedings of PSFVIP-4 F4021*
- Courtine, S., Spohn, A. (2004). Dynamics of separation bubbles formed on rounded edges. In: 12th International Symposium on Applications of Laser Techniques to Fluid Mechanics. Lisbon, Portugal.
- Lamballais, E., Silvestrini, J., Laizet, S. (2008). "Direct Numerical Simulation of a Separation Bubble on a Rounded Finite-Width Leading Edge". *International Journal of Heat and Fluid Flow*, Vol. 29, No. 3, pp. 612-625.
- Lamballais, E., Silvestrini, J., Laizet, S. (2009). "Influence of Rounded Leading Edge on the Flow Separation BY DNS". 20th International Congress of Mechanical Engineering COBEM 2009.
- Lamballais, E., Silvestrini, J., Laizet, S. (2010). "Direct Numerical Simulation of Flow Separation Behind a Rounded Leading Edge: Study of Curvature Effects". *International Journal of Heat and Fluid Flow*, Vol. 31, pp. 295-306.
- Menter, F. R., 1992, "Influence of Free Stream Values on $k-\omega$ Turbulence Model Predictions", *AIAA Journal*, Vol. 30, No. 6, pp. 1657-1659.
- Menter, F. R., Kuntz, M., Langtry, R., 2003, "Ten Years of Industrial Experience with the SST Turbulence Model", *Proceedings of the 4th International Symposium on Turbulence, Heat and Mass Transfer*, pp. 625-632.
- Rezende, A.L.T., Nieckele, A.O., (2007). "Prediction of the Flow Over a Thin Flat Plate at Shallow Incidence" 19th International Congress of Mechanical Engineering COBEM 2007.

W. Miranda, A. Rezende
Reynolds Averaged Navier-Stokes (RANS) Numerical Simulation of a Separation Bubble on a Rounded Edge

Yang Z. & Voke P.R. (2001). "Large-eddy simulation of boundary-layer separation and transition at a change of surface curvature" in *Journal of Fluid Mechanics*, pp. 305-333.

RESPONSIBILITY NOTICE

The authors are the only responsible for the printed material included in this paper.